

A CRANK-NICOLSON L_1 /PI DIFFERENCE SCHEME FOR NONLINEAR TIME FRACTIONAL INTEGRO-DIFFERENTIAL EQUATION ON GRADED MESHES*

Emadidin Gahalla Mohmed Elmahdi^{1,2} and Jianfei Huang^{1,†}

Abstract In this paper, a Crank-Nicolson L_1 /trapezoidal Product integration (PI) difference scheme is constructed to numerically solve a Volterra-type nonlinear integro-differential equation. Assuming the exact solution exhibits a weak singularity at $t = 0$, the convergence order of the fully discrete scheme is $\mathcal{O}(N^{-\min\{r\sigma, 2-\alpha, 2\}} + M^{-2})$, and the stability is analyzed using an improved Grönwall inequality in terms of the L^2 -norm. Finally, the theoretical results are verified by numerical experiments.

Keywords Volterra-type integro-differential equations, nonuniform meshes, finite difference scheme, stability and convergence.

MSC(2010) 65M06, 65M12.

1. Introduction

Fractional integro-differential equations have gained prominence over the past two decades due to their widespread applications in fields, such as anomalous diffusion, mechanical systems, viscoelastic materials, biology and signal analysis [13, 19]. The current study investigates the subsequent fractional nonlinear Volterra integro-differential equation (FNVIDE) including singular kernels:

$$\begin{aligned} \frac{\partial \nu(x, t)}{\partial t} + {}^C D_t^\alpha \nu(x, t) &= {}_0 J_t^\beta \frac{\partial^2 \nu(x, t)}{\partial x^2} + g(\nu(x, t)) + f(x, t), \\ \nu(x, 0) &= 0, \quad x \in (0, L), \\ \nu(0, t) = \nu(L, t) &= 0, \quad t \in (0, T], \end{aligned} \quad (1.1)$$

where $f(x, t)$ is a known function, ${}^C D_t^\alpha \nu(x, t)$ and ${}_0 J_t^\beta \nu(x, t)$ denote the temporal Caputo derivative with order $0 < \alpha < 1$ and the Riemann-Liouville integral operator of order $0 \leq \beta \leq 1$, respectively, defined as

$${}^C D_t^\alpha \nu(x, t) = \int_0^t \bar{\omega}_{1-\alpha}^{(t-s)} \frac{\partial \nu(x, s)}{\partial s} ds, \quad \text{where } \bar{\omega}_\alpha^{(t)} = \frac{t^{\alpha-1}}{\Gamma(\alpha)} \quad (1.2)$$

[†]The corresponding author.

¹College of Mathematical Sciences, Yangzhou University, 225002 Yangzhou, China

²Faculty of Education, University of Khartoum, P. O. Box 321 Khartoum, Sudan

*The authors were supported by Natural Science Foundation of Jiangsu Province of China (Grant No. BK20201427) and by National Natural Science Foundation of China (Grant No. 11701502).

Email: emadgahalla11@gmail.com(E. G. M. Elmahdi), jfhuang@lsec.cc.ac.cn(J. Huang)

and

$${}_0J_t^\beta \nu(x, t) = \int_0^t \bar{\omega}_\beta^{(t-s)} \nu(x, s) ds.$$

In the present study, we claim that the solution $\nu(x, t)$ fulfills the following regularity assumption:

$$\left| \frac{\partial^p \nu(x, t)}{\partial t^p} \right| \leq C (1 + t^{\sigma-p}), \quad \sigma \in (0, 1), \text{ and } p = 1, 2, \quad (1.3)$$

where σ is a regularity parameter, dependent on α and β .

Numerical research of various versions of Eq. (1.1), specifically for the scenario when $\beta = 0$ (fractional mobile/immobile equations FMIMEs) and the fractional diffusion equations FDEs (excluding $\frac{\partial \nu}{\partial t}$ and $\beta = 0$), in both linear and nonlinear frameworks, have been thoroughly analyzed in the literature (see, for instance, [1, 4, 6, 8, 29]). Qiao and Cheng [14] handled 2D variable FMIMEs with the $L1$ finite difference method on uniform meshes. The application of an averaged $L1$ technique for solving nonlinear FMIMEs on nonuniform domains has been analyzed by Yu and Chen in [27] and Tan in [21]. For linear FDEs, the authors in [23, 26] examined an α -robust analysis for the developed schemes. Wang and Sun [25] constructed an $L1$ -type method on nonuniform grids to solve a category of variable-coefficient Caputo-Hadamard FDEs. The stability and convergence of the suggested methods were rigorously shown. Zhu and Xu [28] employed a combination of temporal nonuniform meshes and the spectral method to numerically solve FDEs on unbounded spatial domains. Consequently, this motivates us to examine and analyze a comprehensive framework including all the scenarios previously discussed.

Recently, there has been considerable research on linear FVIDEs (see, for instance, [3, 9, 15, 16, 18, 22]), but comparatively little attention has been devoted to the nonlinear case [2, 10, 17, 20]. In [20], Sunthrayuth et al. constructed a linearized scheme to solve a type of FNVIDEs via a Chebyshev pseudospectral method. Kumar and Gupta [10] implemented fractional-order Lagrange polynomials to introduce and analyze a numerical scheme for solving a type of FNVIDEs. In [17], Saini et al. presented a stable iterative method with convergence order $\mathcal{O}(\tau^{2-\alpha})$ to handle a class of FNVIDEs, while the nonlinear term was treated by the Daftardar-Gejji and Jafari method. Behera and Saha Ray in [2], presented a scheme based on Taylor wavelets technique for solving linear and nonlinear fractional Volterra-Fredholm integro-differential equations. Here, we present a Crank-Nicolson linearized difference scheme for solving a type of FNVIDEs with initial singularity at $t = 0$. We approximate the Caputo derivative and the Riemann-Liouville fractional integral over time by combining the $L1$ scheme and the trapezoidal PI rule on a graded mesh with the Crank-Nicolson method. The fractional central difference formula is utilized to build a full discrete difference scheme. Ultimately, it is shown that the proposed scheme is stable and convergent, with convergence orders of $\mathcal{O}(N^{-\min\{r\sigma, 2-\alpha, 2\}} + M^{-2})$.

The next sections of this paper are organized as follows: Section 2 delineates several practical lemmas and preparatory concepts. In Section 3, a finite difference scheme is formulated. The stability and convergence of the proposed method are explained in Section 4. Alongside the theoretical results, numerical experiments are showcased in Section 5. A succinct summary is given in Section 6.

2. Preliminaries

This section introduces fundamental definitions, significant notations, and key lemmas for constructing and analyzing the difference scheme for problem (1.1).

For positive integer M , let $h = L/M$, $\{x_i = ih\}_{i=0}^M$. Let N be a positive integer, we divide the interval $[0, T]$ into N sub-intervals with $\epsilon_n = \{t_0, \dots, t_N | 0 = t_0 < t_1 < \dots < t_N = T\}$ by $\{t_k = T(k/N)^r\}_{k=0}^N$, where $r \geq 1$, denote the time step as $\tau_k = t_k - t_{k-1}$ and $t_{k-1/2} = (t_k + t_{k-1})/2$.

For any grid point $\{\nu_i^n\}_{i=1}^{M-1}$, we set

$$\delta_x^2 \nu_i^n = \frac{\nu_{i-1}^n - 2\nu_i^n + \nu_{i+1}^n}{h^2} \approx \frac{\partial^2 \nu(x_i, t_n)}{\partial x^2}.$$

Lemma 2.1. ([24], Eq. (2.1)) For $n = 1, 2, \dots, N$. One has

$${}_0^C D_t^\alpha \nu(t_k) = \sum_{k=1}^n c_{n-k}^{(\alpha)} \left(\frac{\nu(t_k) - \nu(t_{k-1})}{\tau_k} \right) + (R_t^\alpha),$$

with

$$c_{n-k}^{(\alpha)} = \frac{1}{\Gamma(2-\alpha)} \begin{cases} (t_n - t_{k-1})^{1-\alpha}, & \text{if } k = n, \\ (t_n - t_{k-1})^{1-\alpha} - (t_n - t_k)^{1-\alpha}, & \text{if } k = 1, 2, \dots, n-1. \end{cases}$$

Lemma 2.2. ([24], Lemma 2.2) For $n \geq 1$ and under assumption (1.3), then

$$\sum_{k=1}^n |P_{n-k}^{(n)}| (R_t^\alpha)^k \leq CN^{-\min\{r\sigma, 2-\alpha\}},$$

where

$$P_{n-k}^{(n)} = \frac{1}{c_0^{(\alpha)}} \begin{cases} 1, & \text{if } k = n, \\ \sum_{j=k+1}^n (c_{j-k-1}^{(\alpha)} - c_{j-k}^{(\alpha)}) P_{n-j}^{(n)}, & \text{if } k = 1, 2, \dots, n-1, \end{cases}$$

and

$$0 < P_{n-k}^{(n)} < \Gamma(2-\alpha)\tau_k^\alpha, \quad 1 \leq k \leq n.$$

According to [24], we approximate the operator ${}_0 J_t^\beta$ by the following trapezoidal product integral method.

$$\left| {}_0 J_t^\beta \nu(t_n) - \frac{\tau_1^\beta}{\Gamma(\beta+2)} \left(\omega_n \nu(t_0) + \sum_{s=1}^n b_{n,s} \nu(t_s) \right) \right| \leq CN^{\min\{r\sigma, 2\}}, \quad 1 \leq n \leq N, \quad (2.1)$$

where $\omega_n = (n^r - 1)^{\beta+1} - n^{r\beta}(n^r - \beta - 1)$, $b_{n,s} = \phi_{n,s}(\beta, r) - \phi_{n,s+1}(\beta, r)$, and $b_{n,n} = (n^r - (n-1)^r)^\beta$ with $\phi_{n,s}(\beta, r) = \frac{(n^r - (s-1)^r)^{\beta+1} - (n^r - s^r)^{\beta+1}}{s^r - (s-1)^r}$.

Lemma 2.3. Let $0 < \mu \leq 1$ and $\nu(t) = \mathcal{O}(t^\sigma)$ satisfies $\nu_{tt}(t) \leq C(1 + t^{\sigma-2})$, then the following results

$$\begin{aligned} \nu(t_{n-\frac{1}{2}}) &= \frac{\nu(t_n) + \nu(t_{n-1})}{2} + \mathcal{O}\left(t_{n-\frac{1}{2}}^{\sigma-2} \tau_n^2\right), \\ {}_0^C D_t^\mu \nu(t_{n-\frac{1}{2}}) &= \frac{{}_0^C D_t^\mu \nu(t_n) + {}_0^C D_t^\mu \nu(t_{n-1})}{2} + \mathcal{O}\left(t_{n-\frac{1}{2}}^{\sigma-\mu-2} \tau_n^2\right), \end{aligned}$$

and

$${}_0J_t^\mu \nu(t_{n-\frac{1}{2}}) = \frac{{}_0J_t^\mu \nu(t_n) + {}_0J_t^\mu \nu(t_{n-1})}{2} + \mathcal{O}\left(t_{n-\frac{1}{2}}^{\sigma+\mu-2} \tau_n^2\right)$$

hold.

Proof. Using Taylor expansion, we have

$$(t_{n-1})^\sigma = \left(t_{n-\frac{1}{2}}\right)^\sigma - \frac{\tau_n}{2} \left(\left(t_{n-\frac{1}{2}}\right)^\sigma\right)' + \frac{\tau_n^2}{8} \int_0^1 \nu''\left(t_{n-\frac{1}{2}} - \frac{\mu\tau_n}{2}\right) (1-\mu) d\mu \quad (2.2)$$

and

$$(t_n)^\sigma = \left(t_{n-\frac{1}{2}}\right)^\sigma + \frac{\tau_n}{2} \left(\left(t_{n-\frac{1}{2}}\right)^\sigma\right)' + \frac{\tau_n^2}{8} \int_0^1 \nu''\left(t_{n-\frac{1}{2}} + \frac{\mu\tau_n}{2}\right) (1-\mu) d\mu. \quad (2.3)$$

From Eqs. (2.2) and (2.3), we have

$$\frac{(t_n)^\sigma + (t_{n-1})^\sigma}{2} = \left(t_{n-\frac{1}{2}}\right)^\sigma + \mathcal{O}\left(t_{n-\frac{1}{2}}^{\sigma-2} \tau_n^2\right).$$

We easily deduce that

$$\begin{aligned} {}_0^C D_t^\mu \nu(t_{n-\frac{1}{2}}) &= \mathcal{O}\left(t_{n-\frac{1}{2}}\right)^{\sigma-\mu} \\ &= \frac{(t_n)^{\sigma-\mu} + (t_{n-1})^{\sigma-\mu}}{2} + \mathcal{O}\left(t_{n-\frac{1}{2}}^{\sigma-\mu-2} \tau_n^2\right) \\ &= \frac{{}_0^C D_t^\mu \nu(t_n) + {}_0^C D_t^\mu \nu(t_{n-1})}{2} + \mathcal{O}\left(t_{n-\frac{1}{2}}^{\sigma+\mu-2} \tau_n^2\right). \end{aligned}$$

Similarly,

$${}_0J_t^\mu \nu(t_{n-\frac{1}{2}}) = \frac{{}_0J_t^\mu \nu(t_n) + {}_0J_t^\mu \nu(t_{n-1})}{2} + \mathcal{O}\left(t_{n-\frac{1}{2}}^{\sigma+\mu-2} \tau_n^2\right),$$

this completes the proof. \square

Lemma 2.4. ([7], Lemma 2.6) Suppose $\nu(t)$ satisfies the assumption (1.3), then the following approximation holds

$$\nu(t_n) = 2\nu(t_{n-1}) - \nu(t_{n-2}) + \mathcal{O}(N^{-r\sigma}).$$

3. Derivation of a finite difference scheme

In this section, we construct a Crank-Nicolson $L1/PI$ method on nonuniform meshes, following the regularity assumption (1.3).

Applying the Crank-Nicolson technique and Lemma 2.3, we get

$$\frac{\nu_t(x_i, t_n) + \nu_t(x_i, t_{n-1})}{2} + \frac{({}_0^C D_t^\alpha \nu(x_i, t_n) + {}_0^C D_t^\alpha \nu(x_i, t_{n-1}))}{2}$$

$$= \frac{{}_0J_{t_n}^\beta \frac{\partial^2 \nu(x_i, t)}{\partial x^2} + {}_0J_{t_{n-1}}^\beta \frac{\partial^2 \nu(x_i, t)}{\partial x^2}}{2} + \frac{g(\nu(x_i, t_n)) + g(\nu(x_i, t_{n-1}))}{2} \\ + f(x_i, t_{n-\frac{1}{2}}) + \mathcal{O}(N^{-2}),$$

where $f(x_i, t_{n-\frac{1}{2}}) = \frac{f(x_i, t_n) + f(x_i, t_{n-1})}{2}$.

Let $\nu(x_i, t_n) = \nu_i^n$. Thus, from Eq. (2.1), Lemma 2.1, Taylor expansion formula to approximate $\nu_t(x, t)$, and the standard difference method to approximate the second-derivative in space, one has

$$\frac{\nu_i^n - \nu_i^{n-1}}{\tau_n} + \frac{1}{2} \left[c_0^{(\alpha)} \frac{\nu_i^n - \nu_i^{n-1}}{\tau_n} + \sum_{k=1}^{n-1} \left(c_{n-k}^{(\alpha)} + c_{n-1-k}^{(\alpha)} \right) \frac{\nu_i^k - \nu_i^{k-1}}{\tau_k} \right] \\ = \frac{\tau_1^\beta}{2\Gamma(\beta+2)} \left[b_{n,n} \delta_x^2 \nu_i^n + \sum_{k=1}^{n-1} (b_{n,k} + b_{n-1,k}) \delta_x^2 \nu_i^k + (\omega_n + \omega_{n-1}) \delta_x^2 \nu_i^0 \right] + \frac{1}{2} [g(\nu_i^n) + g(\nu_i^{n-1})] \\ + f_i^{n-\frac{1}{2}} + (R_x^{\alpha, \beta})_i, \quad (3.1)$$

where $(R_x^{\alpha, \beta})_i = (R_t^\alpha)_i + (R_x^\beta)_i$ and $(R_x^\beta)_i = \mathcal{O}(N^{-\min\{r\sigma, 2\}} + M^{-2})$.

Define

$$\zeta_n = \frac{\omega_n + \omega_{n-1}}{2}, \quad n = 1, 2, \dots, N, \\ \xi_{n-k} = \begin{cases} \frac{b_{n,k}}{2}, & \text{if } k = n, \\ \frac{b_{n,k} + b_{n-1,k}}{2}, & \text{if } k = 1, 2, \dots, n-1, \end{cases}$$

and

$$c_{n-k} = \frac{1}{2} \begin{cases} 2 + c_0^{(\alpha)}, & \text{if } k = n, \\ c_{n-k}^{(\alpha)} + c_{n-1-k}^{(\alpha)}, & \text{if } k = 1, 2, \dots, n-1. \end{cases}$$

So Eq. (3.1) can be expressed as

$${}_0D_t \nu_i^n = \frac{\tau_1^\beta}{\Gamma(\beta+2)} \left(\sum_{k=1}^n \xi_{n-k} \delta_x^2 \nu_i^k + \zeta_n \delta_x^2 \nu_i^0 \right) + \frac{g(\nu_i^n) + g(\nu_i^{n-1})}{2} + f_i^{n-\frac{1}{2}} + (R_x^{\alpha, \beta})_i^n, \quad (3.2)$$

where

$${}_0D_t \nu_i^n := \sum_{k=1}^n c_{n-k} \frac{\nu_i^k - \nu_i^{k-1}}{\tau_k}.$$

From Lemma 2.4 and Taylor expansion theorem we linearize Eq. (3.2) with respect to the unknown variable ν_i^n for $n = 1, 2, \dots, N$ as follows:

$$\left(c_0 - \frac{\tau_1^{\beta+1} \xi_0 \delta_x^2}{\Gamma(\beta+2)} \right) \nu_i^1 = \left(c_0 + \frac{\tau_1^{\beta+1}}{\Gamma(\beta+2)} \zeta_n \delta_x^2 \right) \nu^0 + \tau_1 f_i^{\frac{1}{2}} + \tau_1 (R_x^{\alpha, \beta})_i^1, \quad \text{for } n = 1, \quad (3.3)$$

and

$$\begin{aligned} \left(c_0 - \frac{\tau_n \tau_1^\beta \xi_0 \delta_x^2}{\Gamma(\beta + 2)} \right) \nu_i^n = & c_0 \nu_i^{n-1} - \tau_n \sum_{k=1}^{n-1} c_{n-k} \frac{\nu_i^k - \nu_i^{k-1}}{\tau_k} + \frac{\tau_n \tau_1^\beta}{\Gamma(\beta + 2)} \sum_{k=1}^{n-1} \xi_{n-k} \delta_x^2 \nu_i^k \\ & + \frac{\tau_n \tau_1^\beta}{\Gamma(\beta + 2)} \zeta_n \delta_x^2 \nu^0 + \frac{\tau_n}{2} (g(2\nu_i^{n-1} - \nu_i^{n-2}) + g(\nu_i^{n-1})) + \tau_n f_i^{n-\frac{1}{2}} \\ & + \tau_n \left(R_x^{\alpha, \beta} \right)_i^n, \text{ for } n = 2, 3, \dots, N. \end{aligned} \quad (3.4)$$

By neglecting the truncation error term $\left(R_x^{\alpha, \beta} \right)_i^n$ in Eqs. (3.3), (3.4) and replacing ν_i^n with numerical solution $\tilde{\nu}_i^n$, we obtain

$$\left(c_0 - \frac{\tau_1^{\beta+1} \xi_0 \delta_x^2}{\Gamma(\beta + 2)} \right) \tilde{\nu}_i^1 = \left(c_0 + \frac{\tau_1^{\beta+1}}{\Gamma(\beta + 2)} \zeta_n \delta_x^2 \right) \tilde{\nu}^0 + \tau_1 f_i^{\frac{1}{2}}, \text{ for } n = 1, \quad (3.5)$$

and

$$\begin{aligned} \left(c_0 - \frac{\tau_n \tau_1^\beta \xi_0 \delta_x^2}{\Gamma(\beta + 2)} \right) \tilde{\nu}_i^n = & c_0 \tilde{\nu}_i^{n-1} - \tau_n \sum_{k=1}^{n-1} c_{n-k} \frac{\tilde{\nu}_i^k - \tilde{\nu}_i^{k-1}}{\tau_k} + \frac{\tau_n \tau_1^\beta}{\Gamma(\beta + 2)} \sum_{k=1}^{n-1} \xi_{n-k} \delta_x^2 \tilde{\nu}_i^k \\ & + \frac{\tau_n \tau_1^\beta}{\Gamma(\beta + 2)} \zeta_n \delta_x^2 \tilde{\nu}^0 + \frac{\tau_n}{2} (g(2\tilde{\nu}_i^{n-1} - \tilde{\nu}_i^{n-2}) + g(\tilde{\nu}_i^{n-1})) \\ & + \tau_n f_i^{n-\frac{1}{2}}, \text{ for } n = 2, 3, \dots, N. \end{aligned} \quad (3.6)$$

4. Convergence and stability analysis

This section discusses the stability and convergence of the proposed scheme under an improved Grönwall inequality. First, we define the grid function space as follows:

$$\Theta_h = \{\nu_i | 0 \leq i \leq M \text{ and } \nu_0 = \nu_M = 0\}.$$

For $\nu_i, w_i \in \Theta_h$, we introduce the discrete inner product, L^2 -norm and the semi norm as

$$\langle \nu, w \rangle = h \sum_{i=1}^{M-1} \nu_i w_i, \quad \|\nu\|^2 = \langle \nu, \nu \rangle \quad \text{and} \quad |\nu|_1 = \sqrt{\langle -\delta_x^2 \nu, \nu \rangle} = \sqrt{\langle \delta_x \nu, \delta_x \nu \rangle},$$

respectively.

Lemma 4.1. ([5], Corollary 1) *Consider the sequence $\{\nu^n\}_{n=0}^N$, which represents a mesh function. For all values of n from 1 to N , we have*

$$\sum_{k=1}^n c_{n-k} \frac{\|\nu^k\|^2 - \|\nu^{k-1}\|^2}{\tau_k} \leq 2 \langle \nu^n, {}_0 D_t \nu^n \rangle.$$

The subsequent modified discrete Grönwall inequality constitutes the principal finding in the theoretical investigation. A similar argument in [12] produces the required outcome.

Lemma 4.2. Assume $\{\lambda_n\}_{n=0}^{N-1}$ is a non-negative sequence. Additionally, let the following inequality holds

$$\sum_{k=1}^n c_{n-k} \left((\nu^k)^2 - (\nu^{k-1})^2 \right) \leq \sum_{k=1}^n \lambda_{n-k} \nu^k \nu^n + \nu^n \eta^n + (\phi^n)^2 \text{ for } 1 \leq n \leq N, \quad (4.1)$$

where $\{\nu^n, \eta^n, \phi^n | 1 \leq n \leq N\}$ are non-negative sequences. If there exists a constant Λ independent of step sizes satisfies $\Lambda \geq \sum_{l=0}^{N-1} \lambda_l$ and the maximum step size fulfills

$$\max_{1 \leq n \leq N} \tau_n \leq \frac{1}{\sqrt[\alpha]{2\pi_A \Gamma(2-\alpha) \Lambda}},$$

then

$$\nu^n \leq 2E_\alpha(2 \max(1, \rho) \pi_A \Lambda t_n^\alpha) \left(\nu^0 + \max_{1 \leq k \leq n} \sum_{j=1}^k P_{k-j}^{(k)} (\eta^j + \phi^j) \right) \quad (4.2)$$

holds, where E_α is the Mittag-Leffler function, $\pi_A > 0$, and $\frac{\tau_n}{\tau_{n+1}} \leq \rho$ for $1 \leq n \leq N$.

Lemma 4.3. ([24], Lemma 2.2) Under the assumption (1.3), the following result

$$\sum_{j=1}^n P_{n-j}^{(n)} |R_t^\alpha| \leq C N^{-\min\{r\sigma, 2-\alpha\}}$$

holds.

Lemma 4.4. ([11], Eq. (1.8)) For $n = 1, 2, \dots, N$, one has

$$\sum_{j=1}^n P_{n-j}^{(n)} \leq \frac{11t_n^\alpha}{4\Gamma(1+\alpha)}.$$

Theorem 4.1. Let $\nu(x, t)$ be the exact solution of problem (1.1) and $\{\tilde{\nu}_i^n\}_{i=1}^M$ be the numerical solution of schemes (3.5) and (3.6). If

$$\max_{1 \leq n \leq N} \tau_n \leq \frac{1}{\sqrt[\alpha]{2\pi_A \Gamma(2-\alpha) \Lambda}},$$

then, it holds for $1 \leq n \leq N$ that

$$\|e^n\| = \|\nu^n - \tilde{\nu}^n\| \leq C \left(N^{-\min\{r\sigma, 2-\alpha\}} + M^{-2} \right).$$

Proof. From Eqs. (3.6) and (3.4), we have

$$\begin{aligned} {}_0D_t e_i^n &= \frac{\tau_1^\beta}{\Gamma(\beta+2)} \left(\zeta_n \delta_x^{\beta_2} e_i^0 + \sum_{k=1}^n \xi_{n-k} \delta_x^2 e_i^k \right) \\ &\quad + \frac{g(2\nu_i^{n-1} - \nu_i^{n-2}) - g(2\tilde{\nu}_i^{n-1} - \tilde{\nu}_i^{n-2}) + g(\nu_i^{n-1}) - g(\tilde{\nu}_i^{n-1})}{2} + \left(R_x^{\alpha, \beta} \right)_i^n. \end{aligned}$$

Since $e_i^0 = 0$ for $0 \leq i \leq M$, the above equation becomes

$$\begin{aligned} {}_0D_t e_i^n &= \frac{\tau_1^\beta}{\Gamma(\beta+2)} \sum_{k=1}^n \xi_{n-k} \delta_x^2 e_i^k \\ &\quad + \frac{g(2\nu_i^{n-1} - \nu_i^{n-2}) - g(2\tilde{\nu}_i^{n-1} - \tilde{\nu}_i^{n-2}) + g(\nu_i^{n-1}) - g(\tilde{\nu}_i^{n-1})}{2} + \left(R_x^{\alpha,\beta}\right)_i^n. \end{aligned}$$

Multiplying the above equation by he_i^n and summing over $1 \leq i \leq M-1$, we obtain

$$\begin{aligned} \langle {}_0D_t e^n, e^n \rangle &= \frac{\tau_1^\beta}{\Gamma(\beta+2)} \sum_{k=1}^n \xi_{n-k} \langle \delta_x^2 e^k, e^n \rangle \\ &\quad + \frac{\langle g(2\nu^{n-1} - \nu^{n-2}) - g(2\tilde{\nu}^{n-1} - \tilde{\nu}^{n-2}), e^n \rangle + \langle g(\nu^{n-1}) - g(\tilde{\nu}^{n-1}), e^n \rangle}{2} \\ &\quad + \langle \left(R_x^{\alpha,\beta}\right)^n, e^n \rangle. \end{aligned} \quad (4.3)$$

From Lipschitz condition with respect to the unknown ν and Lemma 4.1, one has

$${}_0D_t \|e^n\|^2 \leq \frac{2\tau_1^\beta}{\Gamma(\beta+2)} \sum_{k=1}^n \xi_{n-k} |e^k|_1 |e^n|_1 + (1 + L_P) \|e^n\|^2 + L_P \langle e^{n-1}, e^n \rangle + \left\| \left(R_x^{\alpha,\beta}\right)^n \right\|^2.$$

Assume that $\|e^P\| = \max_{0 \leq n \leq N}$, then it holds

$${}_0D_t \|e^P\|^2 \leq \frac{2\tau_1^\beta}{\Gamma(\beta+2)} \sum_{k=1}^P \xi_{n-k} |e^k|_1 |e^P|_1 + (1 + 2L_P) \|e^P\|^2 + \left\| \left(R_x^{\alpha,\beta}\right)^P \right\|^2. \quad (4.4)$$

Similarly, from Eqs. (3.3) and (3.5), we obtain

$${}_0D_t \|e^1\|^2 \leq \frac{2\tau_1^\beta}{\Gamma(\beta+2)} \xi_0 |e^1|_1^2 + (1 + 2L_P) \|e^1\|^2 + \left\| \left(R_x^{\alpha,\beta}\right)^1 \right\|^2. \quad (4.5)$$

Summing Eqs. (4.4) and (4.5) gives

$${}_0D_t \|e^P\|^2 \leq \frac{2\tau_1^\beta}{\Gamma(\beta+2)} \sum_{k=1}^P \xi_{P-k} |e^k|_1 |e^P|_1 + (1 + 2L_P) \|e^P\|^2 + \left\| \left(R_x^{\alpha,\beta}\right)^P \right\|^2, \quad (4.6)$$

which has the form of Eq. (4.1) with $\Lambda = 2T^\beta/\Gamma(\beta+1)$. Therefore, applying Lemma 4.3, we obtain

$$\begin{aligned} \|e^P\| &\leq CE_\alpha \left(\frac{4T^\beta \max(1, \rho) \pi_A t_n^\alpha}{\Gamma(\beta+1)} \right) \max_{1 \leq k \leq P} \sum_{j=1}^k P_{k-j}^{(k)} \left\| \left(R_x^{\alpha,\beta}\right)^j \right\| \\ &\leq CE_\alpha \left(\frac{4T^\beta \max(1, \rho) \pi_A t_n^\alpha}{\Gamma(\beta+1)} \right) \max_{1 \leq k \leq P} \sum_{j=1}^k P_{k-j}^{(k)} \left(\|(R_t^\alpha)^j\| + \|(R_x^\beta)^j\| \right). \end{aligned} \quad (4.7)$$

Therefore, from Lemmas 4.3 and 4.4, we obtain

$$\|e^n\| \leq \mathcal{O} \left(N^{-\min\{r\sigma, 2-\alpha, 2\}} + M^{-2} \right).$$

The proof is completed. \square

Theorem 4.2. Assume $\{\tilde{v}^n\}_{i=0}^M$ is the numerical solution of schemes (3.5) and (3.6), it holds

$$\|\tilde{v}^n\| \leq E_\alpha \left(\frac{4T^\beta \max(1, \rho) \pi_A t_n^\alpha}{\Gamma(\beta + 1)} \right) \left(\|\tilde{v}^0\| + \frac{11t_n^\alpha}{4\Gamma(1 + \alpha)} \max_{1 \leq k \leq n} \|f^{k-\frac{1}{2}}\| \right)$$

for $1 \leq n \leq N$.

Proof. Multiplying Eq. (3.6) by $h\tilde{v}_i^n$ and summing over $1 \leq i \leq M - 1$, we obtain

$$\begin{aligned} \langle {}_0D_t \tilde{v}^n, \tilde{v}^n \rangle &= \frac{\tau_1^\beta}{\Gamma(\beta + 2)} \left(\zeta_n \langle \delta_x^2 \tilde{v}^0, \tilde{v}^n \rangle + \sum_{k=1}^n \xi_{n-k} \langle \delta_x^2 \tilde{v}^k, \tilde{v}^n \rangle \right) \\ &\quad + \frac{\langle g(2\tilde{v}_i^{n-1} - \tilde{v}_i^{n-2}) + g(\tilde{v}_i^{n-1}), \tilde{v}_i^n \rangle}{2} + \langle f^{n-\frac{1}{2}}, \tilde{v}^n \rangle. \end{aligned} \quad (4.8)$$

Eq. (1.1) which is characterized by homogeneous initial conditions, resulting in

$$\begin{aligned} \langle {}_0D_t \tilde{v}^n, \tilde{v}^n \rangle &= \frac{\tau_1^\beta}{\Gamma(\beta + 2)} \sum_{k=1}^n \xi_{n-k} \langle \delta_x^2 \tilde{v}^k, \tilde{v}^n \rangle \\ &\quad + \frac{\langle g(2\tilde{v}_i^{n-1} - \tilde{v}_i^{n-2}) + g(\tilde{v}_i^{n-1}), \tilde{v}_i^n \rangle}{2} + \langle f^{n-\frac{1}{2}}, \tilde{v}^n \rangle. \end{aligned} \quad (4.9)$$

Applying similar deductions to get Eq. (4.6), one has

$${}_0D_t \|\tilde{v}^P\|^2 \leq \frac{2\tau_1^\beta}{\Gamma(\beta + 2)} \sum_{k=0}^P \xi_{P-k} |\tilde{v}^k|_1 |\tilde{v}^P|_1 + \|f^{P-\frac{1}{2}}\|^2 + (1 + 2L_P) \|\tilde{v}^P\|^2, \quad (4.10)$$

which has the form of Eq. (4.1) with $\Lambda = \frac{2T^\beta}{\Gamma(\beta+1)}$. Therefore, applying Lemma 4.2 gives

$$\begin{aligned} \|\tilde{v}^P\| &\leq E_\alpha \left(\frac{4T^\beta \max(1, \rho) \pi_A t_P^\alpha}{\Gamma(\beta + 1)} \right) \left(\|\tilde{v}^0\| + \max_{1 \leq k \leq P} \sum_{j=1}^k P_{k-j}^{(k)} + \max_{1 \leq k \leq P} \sum_{j=1}^k P_{k-j}^{(k)} \|f^j\| \right) \\ &\leq E_\alpha \left(\frac{4T^{\beta_1} \max(1, \rho) \pi_A t_P^\alpha}{\Gamma(\beta + 1)} \right) \left(\|\tilde{v}^0\| + \frac{11t_P^\alpha}{4\Gamma(1 + \alpha)} \max_{1 \leq k \leq P} \|f^k\| \right), \end{aligned}$$

where Lemma 4.4 is used. \square

5. Numerical experiments

Here, we conduct numerical experiments to validate the correctness of theoretical analysis and provide our numerical results. All of the computations are performed by using a MATLAB on a computer with Intel(R) Core(TM) i5-8265U CPU 1.60GHz 1.80GHz and 8G Ram.

The following tables display the L^2 -norm errors between the exact and numerical solution, which is denoted by

$$L_{(N,M)}^2 = \max_{0 \leq n \leq N} \|e^n\|$$

and the average CPU time measured in seconds, is expressed by the mean duration. Moreover, the numerical CRs in all possible scenarios are denoted by

$$\text{rate} = \log_2 \left(L_{(N/2, M/2)}^2 / L_{(N, M)}^2 \right) \quad \text{and} \quad \text{rate}_x = \log_2 \left(L_{(N, M/2)}^2 / L_{(N, M)}^2 \right).$$

Example 5.1. Consider Eq. (1.1) with the exact solution $\nu(x, t) = t^\sigma \sin(\pi x)$ and

$$f(x, t) = \sigma t^{\sigma-1} \sin(\pi x) + \frac{\Gamma(\sigma+1)}{\Gamma(\sigma-\alpha+1)} t^{\sigma-\alpha} \sin(\pi x) \\ - \frac{\Gamma(\sigma+1)\pi^2 t^{\sigma+\beta}}{\Gamma(\sigma+\beta+1)} \sin(\pi x) - \nu^2.$$

This experiment evaluates the performance of nonuniform schemes (3.5) and (3.6) by utilizing several graded mesh parameters r , namely $r = 1, \frac{1}{\sigma}, \frac{2-\alpha}{\sigma}$, and 2. The CRs shown in Tables 1 and 2 indicate that schemes (3.5) and (3.6) attain the maximum CR $(2-\alpha)$ for the $L1$ method when $r = \frac{2-\alpha}{\sigma}$, achieving CR σ under uniform meshes ($r = 1$) and has CR $r\sigma$ when $r = 2$. Table 3 illustrates that schemes (5) and (6) achieve second-order precision with the parameters $\alpha = 0.1$, $\sigma = 0.9$, $r = \frac{2-\alpha}{\sigma}$, and 2. This demonstrates that the application of graded mesh significantly enhances the accuracy of the scheme by concentrating a greater density of mesh points at $t = 0$.

Conversely, we evaluate the CR in space as presented in Table 4, maintaining a constant $N = 1000$ and setting $r = \frac{2-\alpha}{\sigma}$, which is characterizes as second-order. The theoretical and experimental findings line up with one another. Finally, Figures 1 and 2 demonstrate that the exact solution $\nu(x, t)$ closely aligns with the linearized difference schemes (3.5) and (3.6) with $N = 100, M = 16, \alpha = 0.4, \sigma = 0.7, \beta = 0.3, r = \frac{2-\alpha}{\sigma}$, and the errors are not significant.

Table 1. The maximum errors and the temporal CR of schemes (3.5) and (3.6).

r	$N = M$	$(\alpha, \sigma, \beta) = (0.3, 0.8, 0.5)$		$(\alpha, \sigma, \beta) = (0.4, 0.7, 0.3)$		$(\alpha, \sigma, \beta) = (0.5, 0.6, 0.1)$		CPU time
		$L^2_{(N,M)}$	rate	$L^2_{(N,M)}$	rate	$L^2_{(N,M)}$	rate	
1	128	3.1576×10^{-3}		7.2614×10^{-3}		1.4296×10^{-2}		0.78
	256	1.9408×10^{-3}	0.7022	4.8237×10^{-3}	0.5901	1.0419×10^{-2}	0.4564	8.72
	512	1.1546×10^{-3}	0.7493	3.0914×10^{-3}	0.6419	7.2564×10^{-3}	0.5219	82.78
	1024	6.7615×10^{-4}	0.7720	1.9469×10^{-3}	0.6671	4.9394×10^{-3}	0.5549	1114.85
Expected CR			0.8		0.7		0.6	
$\frac{1}{\sigma}$	128	1.3754×10^{-3}		2.0726×10^{-3}		2.7438×10^{-3}		0.81
	256	7.0712×10^{-4}	0.9598	1.0558×10^{-3}	0.9732	1.3906×10^{-3}	0.9805	8.73
	512	3.5849×10^{-4}	0.9800	5.3282×10^{-4}	0.9866	7.0006×10^{-4}	0.9902	77.16
	1024	1.8054×10^{-4}	0.9896	2.6772×10^{-4}	0.9929	3.5130×10^{-4}	0.9947	1140.28
Expected CR			1.0		1.0		1.0	
$\frac{2-\alpha}{\sigma}$	128	5.5720×10^{-5}		1.2958×10^{-4}		2.6766×10^{-4}		1.24
	256	1.7183×10^{-5}	1.6972	4.2824×10^{-5}	1.5973	9.4817×10^{-5}	1.4972	8.53
	512	5.2925×10^{-6}	1.6990	1.4137×10^{-5}	1.5990	3.3550×10^{-5}	1.4988	77.43
	1024	1.6294×10^{-6}	1.6996	4.6647×10^{-6}	1.5996	1.1866×10^{-5}	1.4995	1106.69
Expected CR			1.7		1.6		1.5	
2	128	8.8823×10^{-5}		3.3015×10^{-4}		1.0918×10^{-3}		0.54
	256	2.9384×10^{-5}	1.5959	1.2560×10^{-4}	1.3943	4.7811×10^{-4}	1.1913	8.46
	512	9.7033×10^{-6}	1.5985	4.7671×10^{-5}	1.3976	2.0871×10^{-4}	1.1959	80.61
	1024	3.2022×10^{-6}	1.5994	1.8077×10^{-5}	1.3990	9.0972×10^{-5}	1.1980	1105.18
Expected CR			1.6		1.4		1.2	

Table 2. The maximum errors and the temporal CR of schemes (3.5) and (3.6).

r	$N = M$	$(\alpha, \sigma) = (0.2, 0.8)$		$(\alpha, \sigma) = (0.4, 0.6)$		$(\alpha, \sigma) = (0.7, 0.3)$		CPU time
		$L^2_{(N,M)}$	rate	$L^2_{(N,M)}$	rate	$L^2_{(N,M)}$	rate	mean
1	128	2.3468×10^{-3}		1.3977×10^{-2}		1.0142×10^{-1}		0.74
	256	1.7073×10^{-3}	0.4590	1.0408×10^{-3}	0.4254	8.8127×10^{-2}	0.2028	8.45
	512	1.0904×10^{-3}	0.6468	7.3114×10^{-3}	0.5095	7.4542×10^{-2}	0.2415	79.07
	1024	6.5938×10^{-4}	0.7257	4.9900×10^{-3}	0.5511	6.2133×10^{-2}	0.2627	1131.75
Expected CR		0.8		0.6		0.3		
$\frac{1}{\sigma}$	128	1.2729×10^{-3}		2.7666×10^{-3}		4.5174×10^{-3}		0.76
	256	6.8757×10^{-4}	0.8886	1.3993×10^{-3}	0.9834	2.2622×10^{-3}	0.9978	8.36
	512	3.5510×10^{-4}	0.9533	7.0300×10^{-4}	0.9931	1.1319×10^{-3}	0.9989	79.09
	1024	1.8005×10^{-4}	0.9798	3.5223×10^{-4}	0.9970	5.6618×10^{-4}	0.9994	1106.26
Expected CR		1.0		1.0		1.0		
$\frac{2-\alpha}{\sigma}$	128	3.4921×10^{-5}		1.6722×10^{-4}		3.0161×10^{-3}		1.01
	256	1.0043×10^{-5}	1.7979	5.5191×10^{-5}	1.5992	1.3362×10^{-3}	1.1745	8.74
	512	2.8850×10^{-6}	1.7995	1.8209×10^{-5}	1.5998	5.7596×10^{-4}	1.2142	79.59
	1024	8.2857×10^{-7}	1.7999	6.0072×10^{-6}	1.5999	2.4384×10^{-4}	1.2400	1084.29
Expected CR		1.8		1.6		1.3		
2	128	8.8755×10^{-5}		1.0975×10^{-3}		2.9760×10^{-2}		1.01
	256	2.9390×10^{-5}	1.5945	4.7961×10^{-4}	1.1943	1.9808×10^{-2}	0.5873	8.62
	512	9.7055×10^{-6}	1.5985	2.0907×10^{-4}	1.1978	1.3141×10^{-2}	0.5919	77.96
	1024	3.2026×10^{-6}	1.5996	9.1059×10^{-5}	1.1991	8.7017×10^{-3}	0.5947	1093.95
Expected CR		1.6		1.2		0.6		

6. Conclusion remarks

This paper introduces and analyzes a linearized difference method for a class of nonlinear Volterra integro-differential equations that display a weak singularity at the initial time $t = 0$. The $L1$ scheme and trapezoidal PI method are utilised to discretize the Caputo fractional derivative and the Riemann-Liouville integral operator on graded meshes, respectively. Meanwhile, the central difference formula approximates the second-order spatial derivative on uniform meshes. The suggested scheme is demonstrated to be stable and convergent with an order of $\mathcal{O}(N^{-\min\{r\sigma, 2-\alpha, 2\}} + M^{-2})$. The theoretical analysis is supported by the experimental data.

Acknowledgments. This research is supported by Natural Science Foundation of Jiangsu Province of China (Grant No. BK20201427), and by National Natural Science Foundation of China (Grant No. 11701502).

Conflicts of interest. The authors declare that there is no conflict of interest.

Data availability statement. All data in this study were derived from the aforementioned numerical experiment.

Table 3. The maximum errors and the temporal CR of schemes (3.5) and (3.6) with fixed $\sigma = 0.9$ and $\alpha = 0.1$.

r	$N = M$	$\beta = 0.3$		$\beta = 0.5$		$\beta = 0.7$		CPU time
		$L^2_{(N,M)}$	rate	$L^2_{(N,M)}$	rate	$L^2_{(N,M)}$	rate	mean
1	128	8.9170×10^{-4}		9.9529×10^{-4}		1.0359×10^{-3}		0.99
	256	5.5758×10^{-4}	0.6774	5.8224×10^{-4}	0.7735	5.9061×10^{-4}	0.8107	8.28
	512	3.1827×10^{-4}	0.8089	3.2402×10^{-4}	0.8455	3.2571×10^{-4}	0.8586	78.55
	1024	1.7537×10^{-4}	0.8599	1.7669×10^{-4}	0.8709	1.7702×10^{-4}	0.8796	1169.18
Expected CR		0.9		0.9		0.9		
$\frac{1}{\sigma}$	128	6.3638×10^{-4}		6.7323×10^{-4}		6.8634×10^{-4}		1.06
	256	3.4690×10^{-4}	0.8754	3.5424×10^{-4}	0.9264	3.5647×10^{-4}	0.9452	8.33
	512	1.7949×10^{-4}	0.9506	1.8093×10^{-4}	0.9693	1.8130×10^{-4}	0.9754	77.19
	1024	9.1043×10^{-5}	0.9793	9.1321×10^{-5}	0.9864	9.1382×10^{-5}	0.9884	1144.86
Expected CR		1.0		1.0		1.0		
$\frac{2-\alpha}{\sigma}$	128	2.9339×10^{-5}		3.0001×10^{-5}		2.9624×10^{-5}		0.54
	256	7.3132×10^{-6}	2.0043	7.4200×10^{-6}	2.0155	7.1565×10^{-6}	2.0494	8.12
	512	1.8210×10^{-6}	2.0058	1.8322×10^{-6}	2.0179	1.7208×10^{-6}	2.0562	78.35
	1024	4.5305×10^{-7}	2.0070	5.5175×10^{-7}	2.0200	4.1171×10^{-7}	2.0634	1104.97
Expected CR		1.9		1.9		1.9		
2	128	3.0540×10^{-5}		3.1674×10^{-5}		3.2499×10^{-5}		0.58
	256	7.6137×10^{-6}	2.0040	7.8424×10^{-6}	2.0139	7.8901×10^{-6}	2.0423	7.76
	512	1.8958×10^{-6}	2.0058	1.9375×10^{-6}	2.0171	1.9036×10^{-6}	2.0513	77.95
	1024	4.7155×10^{-7}	2.0073	4.7758×10^{-7}	2.0204	4.5596×10^{-7}	2.0617	1093.46
Expected CR		1.8		1.8		1.8		

Table 4. The maximum errors and the spatial CR of schemes (3.5) and (3.6) with fixed $N = 1000$.

M	$(\alpha, \sigma, \beta) = (0.3, 0.8, 0.5)$		$(\alpha, \sigma, \beta) = (0.4, 0.7, 0.3)$		$(\alpha, \sigma, \beta) = (0.5, 0.6, 0.1)$		CPU time
	$L^2_{(N,M)}$	rate _x	$L^2_{(N,M)}$	rate _x	$L^2_{(N,M)}$	rate _x	mean
8	9.8125×10^{-3}		9.4179×10^{-3}		9.1487×10^{-3}		5.35
16	2.4379×10^{-3}	2.0090	2.3395×10^{-3}	2.0092	2.2727×10^{-3}	2.0091	5.57
32	6.0844×10^{-4}	2.0025	5.8380×10^{-4}	2.0027	5.6689×10^{-4}	2.0033	5.80
64	1.5194×10^{-4}	2.0015	1.4573×10^{-4}	2.0021	1.4124×10^{-4}	2.0049	7.75
Expected CR		2.0	2.0		2.0		

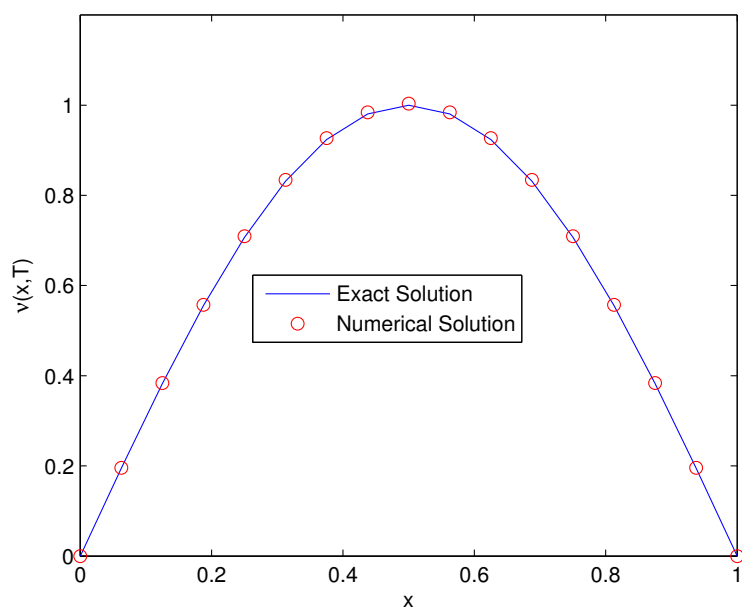


Figure 1. The comparison between the exact solution $\nu(x,t)$ with the numerical schemes (3.5) and (3.6) of problem (1.1).

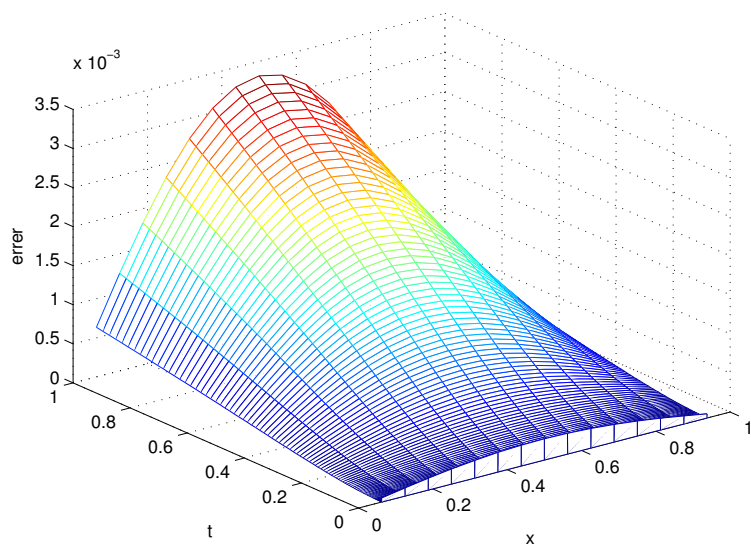


Figure 2. The error surface between the numerical solution and the exact solution of schemes (3.5) and (3.6).

References

- [1] A. A. Alikhanov, P. Yadav, V. K. Singh and M. Shahbazi Asl, *A high-order compact difference scheme for the multi-term time-fractional Sobolev-type convection-diffusion equation*, Appl. Numer. Math., 2025, 44(115), 82–95.
- [2] S. Behera and S. Saha Ray, *A wavelet-based novel technique for linear and nonlinear fractional Volterra-Fredholm integro-differential equations*, Comput. Appl. Math., 2022, 41(1), 1–28.
- [3] F. Boutaous, *Study of a class of fractional order non linear neutral abstract Volterra integro-differential equations with deviated arguments*, Chaos Solit. Fractals, 2024, 187, 115341.
- [4] Y. Cao and Z. Tan, *A fast and high-order localized meshless method for fourth-order time-fractional diffusion equations*, Commun. Nonlinear Sci. Numer. Simul., 2025, 142, 108586.
- [5] H. Chen and M. Stynes, *Error analysis of a second-order method on fitted meshes for a time-fractional diffusion problem*, J. Sci. Comput., 2019, 79(2), 624–647.
- [6] E. G. M. Elmahdi and J. Huang, *A linearized finite difference scheme for time-space fractional non-linear diffusion-wave equations with initial singularity*, Int. J. Nonlinear Sci. Numer. Simul., 2023, 24(6), 1769–1783.
- [7] E. G. M. Elmahdi, Y. Yi and J. Huang, *Two linearized difference schemes on graded meshes for the time-space fractional nonlinear diffusion-wave equation with an initial singularity*, Phys. Scr., 2025, 100(1), 015215.
- [8] Y. Jiang, H. Chen, T. Sun and C. Huang, *Efficient L1-ADI finite difference method for the two-dimensional nonlinear time-fractional diffusion equation*, Appl. Math. Comput., 2024, 471, 128609.
- [9] S. Kumar, S. Das and V. K. Singh, *Product integration techniques for generalized fractional integro-differential equations*, Z. Angew. Math. Phys., 2025, 76(1), 1–30.
- [10] S. Kumar and V. Gupta, *An approach based on fractional-order Lagrange polynomials for the numerical approximation of fractional order nonlinear Volterra-Fredholm integro-differential equations*, J. Appl. Math. Comput., 2023, 69(1), 251–272.
- [11] H. L. Liao, W. McLean and J. Zhang, *A second-order scheme with nonuniform time steps for a linear reaction-subdiffusion problem*, Commun. Comput. Phys., 2021, 30(2), 567–601.
- [12] H. L. Liao, W. McLean and J. Zhang, *A discrete Grönwall inequality with applications to numerical schemes for subdiffusion problems*, SIAM J. Numer. Anal., 2019, 57(1), 218–237.
- [13] S. Patnaik, J. P. Holkamp and F. Semperlotti, *Applications of variable-order fractional operators: A review*, Proc. R. Soc. Lond. Ser. A Math. Phys. Eng. Sci., 2020, 476(2234), 20190498.
- [14] H. Qiao and A. Cheng, *A fast finite difference method for 2D time variable fractional mobile/immobile equation*, J. Appl. Math. Comput., 2024, 70(1), 551–577.
- [15] Y. Rostami, *New technique for solving system of variable-order fractional partial integro-differential equations*, Comput. Math. Phys., 2025, 65(2), 270–289.
- [16] Ruby and M. Mandal, *Convergence analysis and numerical implementation of projection methods for solving classical and fractional Volterra integro-differential equations*, Math. Comput. Simul., 2024, 225, 889–913.

- [17] G. Saini, B. Ghosh, S. Chand and J. Mohapatra, *An iterative-based difference scheme for nonlinear fractional integro-differential equations of Volterra type*, Partial Differ. Equ. Appl. Math., 2025, 13, 101138.
- [18] S. Santra and J. Mohapatra, *Numerical analysis of volterra integro-differential equations with Caputo fractional derivative*, Iran. J. Sci. Technol. Trans. Sci., 2021, 45(5), 1815–1824.
- [19] M. V. Shitikova, *Fractional operator viscoelastic models in dynamic problems of mechanics of solids: A review*, Mech. Solids, 2022, 57(5), 1–33.
- [20] P. Sunthrayuth, R. Ullah, A. Khan, R. Shah, J. Kaffle, I. Mahariq and F. Jarad, *Numerical analysis of the fractional-order nonlinear system of volterra integro-differential equations*, J. Funct. Spaces, 2021, 2021, 5536569.
- [21] Z. Tan, *Second-order non-uniform and fast two-grid finite element methods for non-linear time/fractional mobile/immobile equations with weak regularity*, Appl. Math. Comput., 2025, 486, 129043.
- [22] S. S. Tantawy, *Solving linear systems of fractional integro-differential equations by Haar and Legendre wavelets techniques*, Partial Differ. Equ. Appl. Math., 2024, 10, 100683.
- [23] Z. Wang, *$L1/LDG$ method for Caputo-Hadamard time fractional diffusion equation*, Commun. Appl. Math. Comput., 2025, 7(1), 203–227.
- [24] Z. Wang, D. Cen and Y. Mo, *Sharp error estimate of a compact $L1$ -ADI scheme for the two-dimensional time-fractional integro-differential equation with singular kernels*, Appl. Numer Math., 2021, 159, 190–203.
- [25] Z. Wang and L. Sun, *A numerical approximation for the Caputo-Hadamard derivative and its application in time-fractional variable-coefficient diffusion equation*, Discrete Contin. Dyn. Syst., 2024, 17(6), 2679–2705.
- [26] Y. Yang, J. Huang and H. Li, *An α -robust analysis of finite element method for space-time fractional diffusion equation*, Numer. Algorithms, 2025, 98(1), 165–190.
- [27] F. Yu and M. Chen, *Second-order error analysis for fractal mobile/immobile Allen-Cahn equation on graded meshes*, J. Sci. Comput., 2023, 96(1), 49.
- [28] H. Zhu and C. Xu, *A highly efficient numerical method for the time-fractional diffusion equation on unbounded domains*, J. Sci. Comput., 2024, 99(1), 1–34.
- [29] L. Zou and Y. Zhang, *Numerical solutions of multi-term fractional reaction-diffusion equations*, AIMS Math., 2025, 10(1), 777–792.

Received April 2025; Accepted August 2025; Available online August 2025.